Schizophrenia Bulletin Open
https://doi.org/10.1093/schizbullopen/sgac055

A Possible White Matter Compensating Mechanism in the Brain of Relatives of People Affected by Psychosis Inferred from Repeated Long-Term DTI Scans

Yaron Caspi[*,1,2]

[1]UMC Utrecht Brain Center, Department of Psychiatry, University Medical Center, Utrecht, The Netherlands
Present address: [2]Department of Psychology, National Taiwan University, Taiwan

*To whom correspondence should be addressed; Department of Psychiatry, University Medical Center, Heidelberglaan 100 3584 CX Utrecht, The Netherlands; tel: 886-2-33664463, e-mail: ycaspi@ntu.edu.tw

Background and Hypothesis: **An existing model suggests that some brain features of relatives of people affected by psychosis can be distinguished from both the probands and a control group. Such findings can be interpreted as representing a compensating mechanism.** ***Study Design:*** **We studied white matter features using diffusion tensor imaging in a cohort of 82 people affected by psychosis, 122 of their first-degree relatives, and 89 control subjects that were scanned between two to three times with an interval of approximately 3 years between consecutive scans. We measured both fractional anisotropy and other standard diffusivity measures such as axial diffusivity. Additionally, we calculated standard connectivity measures such as path length based on probabilistic or deterministic tractography. Finally, by averaging the values of the different measures over the two or three consecutive scans, we studied epoch-averagely the difference between these three groups.** ***Study Results:*** **For several tracts and several connectivity measures, the relatives showed distinct features from both the probands and the control groups. In those cases, the relatives did not necessarily score between the probands and the control group. An aggregate analysis in the form of a group-dependent score for the different modes of the analysis (e.g., for fractional anisotropy) supported this observation.** ***Conclusions:*** **We interpret these results as evidence supporting a compensation mechanism in the brain of relatives that may be related to resilience that some of them exhibit in the face of the genetic risk they have for being affected by psychosis.**

Key words: psychosis/first-degree relatives/familial risk/diffusion tensor imaging/connectivity/resilience

Introduction

Extensive findings concerning subjects diagnosed with psychosis (D), their first-degree relatives, and the general population fit the "Familial Risk" model.[1] According to this model, some alterations in the brain of the D group will be detected to a lesser extent in the brain of their relatives.[2] These brain abnormalities would represent the increased liability of the relatives to be affected by psychosis.[3,4]

An alternative model suggests that the average brain of relatives is different from the average brain of the affected probands but also different from the average brain of the general population. In its extreme form, this model suggests an inverse U-shape relationship between the genetic liability to psychosis and brain functionality.[5,6] A more moderate framework ("Compensating Mechanisms") is based on the same assumption. However, it interprets these features as the manifestations of compensatory, protective, or resilience mechanisms that enable relatives to function similarly to subjects from the general population. Note that these two models are not mutually exclusive, as some brain features might follow one of the models while other features follow the second one. Moreover, different relatives groups (monozygotic twins, dizygotic twins, siblings, parents, etc.) might exhibit different familial risk or compensation features due to a different genetic load and environmental factors.

Many studies[7–10] support the "Familial Risk" model, for example, concerning white matter (WM) volume[11] or specific WM tracts.[12,13] There is also widespread evidence for abnormalities in WM among people at high risk for psychosis (not necessarily as part of the relatives' group).[14–16]

Despite the stress on risk factors in psychiatry, the interest in understanding resilience or plasticity mechanisms currently increases.[17–20] Therefore, it is valuable to consider evidence supporting the "Compensating Mechanisms" model or evidence suggesting a more complex state of affairs than a simple familial risk. Indeed, several studies suggested the latter case. For example, several studies

showed no correlation between Polygenic Risk Score for Schizophrenia (szPRS) and brain abnormalities.[21–23] Similarly, while excessive abnormalities might be expected at old age with increased szPRS, several graph-theoretical measures were not associated with szPRS.[24]

Some studies also showed both vulnerability and resilience patterns in the brain of relatives.[25,26] For example, siblings showed stronger structural connectivity compared to a control group in some brain regions, while in other regions, both the siblings and the affected probands showed similar patterns of vulnerability.[27]

Finally, some studies also suggested the existence of a compensation mechanism among siblings. For example, an increased Fractional Anisotropy (FA) value was observed among adolescent relatives in the tracts connecting the nucleus accumbens compared to a control group.[28] Similarly, reduced szPRS was associated with enlarged total ventricles' volume for subjects with relatively low cortisol levels and not a reduced one.[29]

The Genetic Risk and Outcomes of Psychosis (GROUP) cohort provides an intriguing option to study the possibility of a compensation mechanism in the brain of relatives. The reason is that this cohort consists of several repeated measurements taken over several years (several epochs of measurements) and studied as subjects both people diagnosed with psychosis, their relatives, and a control group. Previous structural research in this cohort discussed the possibility of a compensatory mechanism in some WM tracts in the brain of relatives.[30] Similarly, another study of the first wave of that cohort suggested such a mechanism based on the assessment of the tissue-FA.[31] Nevertheless, whether an indication of a compensation mechanism in the brain of relatives from this cohort exists remains an open question. To search for an indication of such a mechanism, we investigated WM in the brain of relatives based on Diffusion Tensor Imaging (DTI) measurements.[32] We studied the epoch-averaged behavior over two to three waves of the GROUP cohort concerning (1) various forms of diffusivity measures such as Fractional Anisotropy (FA) and (2) various structural connectivity measures. In addition, we carried out a linear mixed model analysis of the longitudinal aspect of those measures. Our working hypothesis for this study was that a compensating mechanism in the brain of the relatives group would be found.

Methods

We used the data from the three epochs (i.e., waves) of the Utrecht site GROUP cohort.[33] This cohort contains DTI measurements of three groups of people—a diagnosed group, a control group, and relatives (all siblings). Altogether, we have analyzed data of 82, 89, and 122 subjects from the diagnosed, control, and relatives groups (15, 47, 71 females) that had two or three consecutive scans and that passed our quality-control procedure (see below). For general characteristics, see tables S1–S3 and figures S1–S3 of the supporting information (SI). Note that the percentage of females is different between the D and the other groups (χ^2 test P-value for the control-diagnosed groups 5.9e-06; χ^2 test P-value for the relatives-diagnosed groups 3.5e-08) but not between the control and relatives groups (χ^2 test P-value 0.5234). Hence, we have corrected the results for sex as is detailed below.

For image acquisition, see[30] and the Supporting Text in the SI. For the image processing pipeline, see figure 1a and the Supporting Text. Since we used an extensive data analysis procedure as is described below, for the clarity of reading we provide, in addition, a detailed graphical presentation of the data analysis pipeline in Supplementary figure S4 in the form of a flowchart.

For each individual and each epoch of the study, the processing pipeline resulted in a set of diffusivity measures (for 48 different tracts) for four different diffusivity modes [FA, Mean Diffusivity (MD), Axial Diffusivity (AD), and Radial Diffusivity (RD)], and a set of connectivity measures (thirteen graph matrix measures—see the SI[34–36]) for four different modes of connectivity matrix calculation. These modes are: (a) connectivity matrix based on a deterministic tracking algorithm; (b) connectivity matrix based on a probabilistic tracking algorithm; (c) connectivity matrix based on sampling FA along the tracts obtained from the deterministic algorithm; (d) connectivity matrix based on sampling FA along the tracts obtained from the probabilistic algorithm.

Before analysis, we applied a two-layered quality-control procedure to reject unreliable scans—see figure S5 and the Supporting Text in the SI for further details.

All data analysis was carried using the statistical computing environment R.[37]

Epoch-Averaged Data Analysis

Data Preparation

To identify the stable component behavior over all epochs of the study, the average value for each subject and for each measure was calculated over two or three measurements (see table S3 of the SI). These average values for each measure (denoted with subscript m) as well as the average age (denoted age_m) at the time of measurement were used for the epoch-averaged analysis.

We added a partial least square (PLS) analysis (using the pls package of R) separately to the diffusivity and connectivity sets.[38] PLS is a statistical method similar to principal components analysis that identifies latent variables which are (optimal) linear combinations of variables. A standard method of PLS calculation include identifying the best number of components for the PLS calculation followed by ranking of the loading of each variable into these components. In this PLS calculation, we involved the number of components that minimized the root-mean-square (RMS) mocked Group label

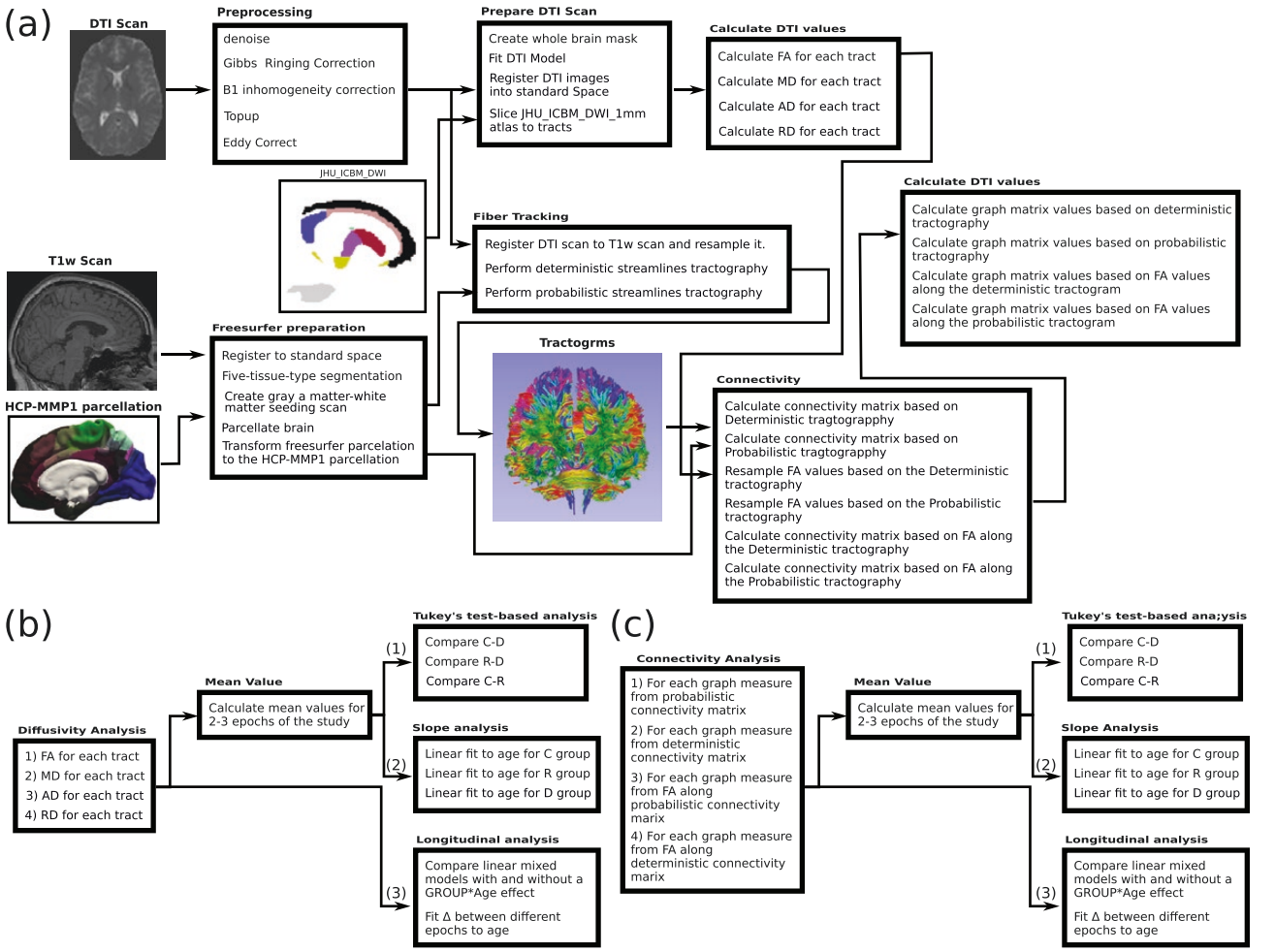

Fig. 1. Summary of processing and analysis pipelines. (a) Summary of the computational pipeline used to processes the scans and calculate form them diffusivity and connectivity values. For calculation we used FSL,[73] MRtrix[74] and FreeSurfer.[75] First, scans are pre-processed to remove distortion. Next, a DTI model is built, and the FA, MD, AD, and RD are calculated for each tract from the JHU ICBM MW atlas. In parallel, tractography is conducted using both deterministic and probabilistic tractography algorithms, and connectivity matrices are calculated based on the HCP-MMP1 parcellation atlas (using the corresponding T1w scan processed via FreeSurfer).[76] In addition, connectivity matrices are calculated for both algorithms by sampling FA values along the tracts. From these four connectivity matrices, several graph matrix measures are calculated (see the Supporting Text at the SI). (b) and (c) Scheme for diffusivity and connectivity data analysis. For each connectivity or diffusivity mode, the average values for all available data for each individual were calculated, and an epoch-averaged Tukey's Test Analysis and epoch-averaged slope analysis was carried. In parallel, a longitudinal analysis was carried using a linear mixed model and analyzing the difference of the values (Δ). Note that the outliers filtering step is not shown.

prediction error and used this number for subsequent calculation of the PLS value (see figure S6a, b of the SI). The mocked Group labels were 1—for controls, 2—for relatives, 3—for the D group. Next, with this number of components, we calculated a loading factor for each measure. Usually, the sorted loading values showed an elbow-like behavior with some variables having a high loading and some having a low loading—see an example of a scree-plot in figure S6c of the SI. To choose variables with high loading and obtaining the relevant measures for the PLS calculation, we fitted the four measures with the highest loading and the ten measures with the smallest loading to straight lines and found the intersect of these two fitted lines (see figure S6c, d of the SI). Measures with loading higher than the intersect value were included in the calculation of the PLS average. For the diffusivity case, the PLS average was the arithmetic mean of all the tracts with the accepted loading. For the connectivity case, measures were first normalized by dividing each value by the maximum value for that measure and then averaging the standardized values. For the diffusivity measures, we also included the average FA_m, MD_m, AD_m, and RD_m, over all 48 tracts. Thus, we ended up with 50 (48 tracts + PSL average + general average) diffusivity measures for each mode of diffusivity calculation and 14 connectivity measures (13 graph matrix values + PLS average) for each mode of connectivity matrix calculation.

For connectivity measures, we applied an additional preparation step. It is known that many connectivity measures depend on the density.[36,39] Hence, for each connectivity measure (besides density), we constructed a model $Measure_m \sim Density_m$. Next, we checked the model *P*-value. For cases where the model *P*-value was below 0.05, we regressed the density dependency. Consequently, the residuals derived from such regression analysis correcting for density became data in the subsequent epoch-averaged analysis.

For each one of the diffusivity or connectivity measures, we applied two types of epoch-averaged analysis. First, we used analysis of covariance (ANCOVA) followed by Tukey's test analysis. Second, we directly calculated the age-dependent epoch-averaged slope for each group. In both cases, after analyzing each measure separately, we studied the results of all measures together. This was achieved by calculating scoring results for each diffusivity mode and each of the four ways of connectivity matrix calculations according to the formulas described below. Such scoring calculation allows us to identify a general pattern of difference between the three groups. Finally, we studied longitudinal aspects of the data. All those analysis modes are described below.

Tukey's Test Analysis

We compared the distribution of values of each $Measure_m$ and each mode of calculation between the three groups. For this purpose, we used a hierarchical approach. First, to account for the relative incidence of females and males among the three groups, we constructed a linear model for each measure with sex, age, and group labels as covariates. The model had the form: $Measure_m \sim Age_m + GROUP + Sex$. Next, for cases where the model Sex label *P*-value was below 0.1, we equated the average value of the female group to the male group by adding the value of the model Sex label to each female individual. That is, we obtained $Measure_m$ (females, corrected) = $Measure_m$ (females, uncorrected) + Sex.

Next, using the set of corrected data, we compared the three groups by constructing an ANCOVA model of the form $Measure_m \sim Age_m + GROUP$, and running an ANOVA on the GROUP label. Moreover, we used Tukey's test of the ANCOVA model for comparison between the group label values of each two groups. Using the Tukey's test we compared the Control and Diagnosed groups (C-D), Relatives and Diagnosed groups (R-D), and the Control and Relatives groups (C-R). The Tukey's test resulted in *P*-values for the C-D, R-D and C-R comparisons for each measure. These *P*-values were corrected for multiple testing (50 tests for diffusivity and 14 tests for connectivity) using the False Discovery Rate (FDR) method.

Finally, as a Supplementary Test, we used Duncan's test to rank the relative level of each group. This test attributes a level to each group depending on how much is it different from the other two groups. Note that this test suffers from an inflated family-wise Type I error rate. Hence, it was only used as supplementary evidence to support the findings of the Tukey's test.

Tukey's test scoring—We collected all measures with an FDR corrected *P*-value (*q*-value) below 0.05 for score calculations. For each relevant measure from each analysis mode, we matched a score equal to [(0.05—*q*-value) × *M*]. The multiplication factor (*M*) was equal to 1, 0.5, and 1/3 for cases where only one, two, or three of the three group comparisons had a *q*-value below 0.05. The multiplication factor provides a simple way to weight differently cases where only one comparison is meaningful versus those of two or three comparisons. Finally, we summed up the scores for all measures related to each diffusivity or connectivity analysis modes.

Slope Analysis

For the slope analysis, we have used a hierarchical approach. For each measure, we constructed three models (in R notation) (a) a general model: $Measure_m \sim Age_m$; (b) Group-dependent model: $Measure_m \sim Group/Age_m$; (c) Group and Sex model: $Measure_m \sim (Group \times Sex)/Age_m$. Next, we calculated the ANOVA *P*-value between model (a) and the others. For cases that the ANOVA *P*-value was below 0.05, we collected all slope values (for each group or each sex-dependent group) with a *P*-value lower than 0.1. These slope values were incorporated into our slope analysis scores (see below).

Slope analysis scoring—The scoring system was similar to the one for Tukey's test analysis with some modification. In this case, for cases model (b) was the most significant, the score was equal to: [(0.1—$P\text{-value}_{slope}$) × *M*]. The multiplication factor (*M*) was equal to 1, 0.5, 1/3 if the slope *P*-value was below 0.1 for only one, two, or three out of the groups. Note that we chose to work with *P*-values smaller than 0.1 rather than the more common one of 0.05. This difference however is taken into account by the 0.1—*P*-value factor. For cases where females and males were fitted separately [model (c)], the multiplication factor was divided by 2. Finally, we summed up the scores for all measures related to each diffusivity or connectivity mode of analysis.

Longitudinal Data Analysis

To reduce the problem of multiple comparisons, we have used a hierarchical approach, which allowed us to reduce the number of measures taken into account for the FDR *q*-value calculation. First, for each of the diffusivity and connectivity measures, we calculated the age-dependent slope for each individual separately. Next, we draw all slopes for each measure and checked if they show differential age-dependency behavior between the different groups by ANOVA of the three models (similar to the age-dependent

epoch-averaged analysis). Only measures for which at least one group, the males or females separately or together, showed a slope *P*-value below 0.05 at the subjects set level were qualified for the linear mixed model analysis.

For these measures, we compared two longitudinal linear mixed models, (a) a general model with fixed effects for the scanner, sex, age, epoch, and group labels and a random effect for the subject nested in the family label. In R notation this model is: Measure ~ (MRI_Scan + Se x + Age + Epoch + Group) + (1| Family:Subject); and a model (b), similar model to (a) but with an additional fixed-effect of group*age. Namely, Measure ~ (MRI_Sca n + Sex + Age + Epoch + Group + Age*Group) + (1| Family:Subject). In addition, for connectivity measures other than the density, we also added density as an additional fixed-effect factor. Next, we checked that both models converged, and for those models calculated the ANOVA *P*-value between models (a) and (b) to determine if adding the interaction effect resulted in a significantly better fit. This procedure resulted in a set of measures (or an empty set) for each data analysis mode. For each set, we calculate the FDR corrected *q*-value. Finally, for measures that had an ANOVA *q*-value below 0.05, we studied the functional-dependency of $\Delta_{T2\text{-}T1}(\text{Age}) \equiv \text{Value}_{T2}(\text{Age}) - \text{Value}_{T1}(\text{Age})$, where $\text{Value}_{X}(\text{Age})$ is the value of some measure for some individual subject at the *X* epochs of the study [*X* = First (T1), Second (T2), or Third (T3)]. Similarly, we studied $\Delta_{T3\text{-}T2}(\text{Age})$ and $\Delta_{T3\text{-}T1}(\text{Age})$.

Results

Tukey's Test Analysis

Diffusivity Measures.

FA Values Results of Tukey's test comparisons are shown in figure 2 and table S4 of the SI. Only six tracts were identified as having a *q*-value below 0.05. All these tracts had ANOVA FDR corrected *P*-value (*q*-value) below 0.05. These tracts are the body of corpus callosum, middle cerebellar peduncle, uncinate fasciculus left, uncinate fasciculus right, anterior corona radiata right, and the superior fronto occipital fasciculus left. For the four first measures, these tracts had Tukey's test *q*-value below 0.05 only for comparing the control and relatives groups but not between the control and diagnosed groups or relatives and diagnosed groups. Duncan's test labeled the relatives with the diagnosed group for the middle

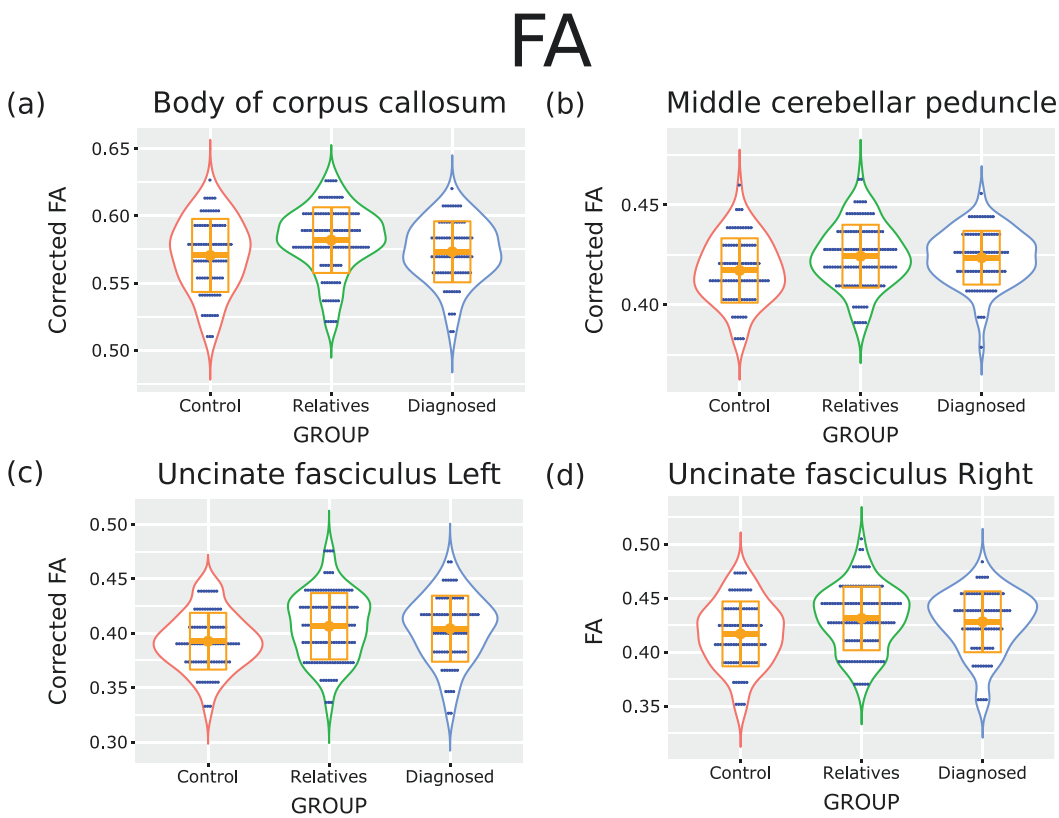

Fig. 2. Tukey's test comparisons analysis of FA results—largest effect. Violin plots for four corrected FA values measures that showed the larges Tukey's test difference (FDR corrected *q*-value below 0.05) when comparing one of the three possible comparisons between the different groups. I.e., the control-diagnosed groups, control-relatives groups, and relative-diagnosed groups. Orange squares represent the median data values, and orange boxes represent SD. For the body of the corpus callosum, the figure represents values after correction for sex and age. For the middle cerebellar peduncle and the left uncinate fasciculus the figures represent values after correction for sex alone. No correction was applied for the right uncinate fasciculus.

cerebellar peduncle, uncinate fasciculus left, and uncinate fasciculus right. For the body of corpus callosum, the relatives were labeled separately from the other two groups. However, as can be seen in figure 2, in all four cases, the relatives had, on average, higher FA values in these tracts than the other two groups.

For the anterior corona radiata right and the superior fronto occipital fasciculus left, the only Tukey's test q-value below 0.05 was for the R-D comparison. In these two cases, Duncan's test also labeled the relatives alone while the control and diagnosed groups were labeled together.

No Tukey's test showed a q-value below 0.05 for the C-D comparison.

When accounting for FDR q-values between 0.05 and 0.1 for the ANOVA and Tukey's test, we identified many more tracts (see table S5 of the SI). In all these cases, it was the comparison between the relatives and control groups that showed Tukey's test q-value below 0.1. Duncan's test labeled the relatives' group as having the most extreme value. This fact suggests a slight tendency for average FA value differences between the control and the relatives groups.

MD, RD, and AD Values No tract had an FDR q-value below 0.05 (or below 0.1) for any of the Tukey's test comparisons between the different groups.

Connectivity Measures

Deterministic Tracts Construction. The Tukey's test comparisons results are shown in Fig. S7 and Table S6 of the SI. Only two measures, the residuals of the assortativity (after density correction), and the PLS average (containing the residuals of the assortativity, residuals of modularity, residuals of the mean participation coefficients, and transitivity) showed a q-value below 0.05 and only for the C-D case. The trivariate ANOVA q-value was also below 0.05. Duncan's test classified the relatives group with the diagnosed group for the PLS average and as an intermediate group between the other two groups for the residuals of the assortativity.

All Other Connectivity Measures. No Tukey's test comparison had a q-value below 0.05 (or below 0.1).

Epoch-Averaged Slope Analysis

The facts that, (1) for FA, we found q-value differences below 0.05 only for Tukey's test comparison of the C-R or R-D groups, (2) these findings were consistent with the previous finding from the first wave of this cohort,[30,31] and (3) many tracts showed q-value between 0.05 and 0.1, inspired us to look more closely into the data using an additional mode of analysis. In this mode of analysis, we analyzed which of the three groups had an epoch-averaged structural age-dependency. The results are detailed below.

Diffusivity Measures

FA Values The epoch-averaged FA slope analysis results are shown in Figs. 3a–d and Table 1. Several tracts had P-value for the age-dependent slope of the fit below 0.1 for at least one of the three groups (control, relatives, or diagnosed). Many of these tracts were previously identified as relevant for psychosis, such as the fornix, body and genu of the corpus callosum (CC), and tracts that radiate from the CC (corona radiata). Also, some thalamic-related tracts and corticospinal tracts (posterior limb of the internal capsule) showed group-dependent age-related change, at least for some sex. Interestingly, in many cases, the relatives group showed a unique epoch-averaged age-dependence behavior in comparison to the control or diagnosed groups.

MD Values The epoch-averaged MD slope analysis results are shown in figure S8 and Table S7 of the SI. Only four tracts showed age-dependent functional-behavior for one or more of the groups and for both sexes or one sex separately. In that case, the relatives group showed the smallest number of tracts with epoch-averaged structural age-dependency behavior.

AD Values The epoch-averaged AD slope analysis results are shown in figure S9 and Table S8 of the SI. Many tracts that were implicated in the FA analysis were also implicated in the AD analysis. However, in this case, values for the age-dependency obtained a P-value below 0.1 only for males or for females separately but not together. Moreover, the control group showed the largest number of tracts with age-dependency, while the diagnosed group showed the smallest number of structural age-dependency behavior.

RD Values The epoch-averaged RD slope analysis results are shown in figure S10 and Table S9 of the SI. Similar to the MD analysis, only a few tracts showed an epoch-averaged age-dependency. These tracts included the fornix and genu of the CC, but also the Cingulum hippocampus and the Pontine crossing tract.

Connectivity Measures

Deterministic Tracts Construction. The epoch-averaged slope analysis results are shown in figure S11 and Table S10 of the SI. The only measure that showed a structural epoch-averaged age-dependent behavior was the residuals of the mean participation coefficients and only for the control group.

FA Values Along Tracts Constructed by a Deterministic Algorithm. The epoch-averaged slope analysis results are shown in figure S12 and Table S11 of the SI. The

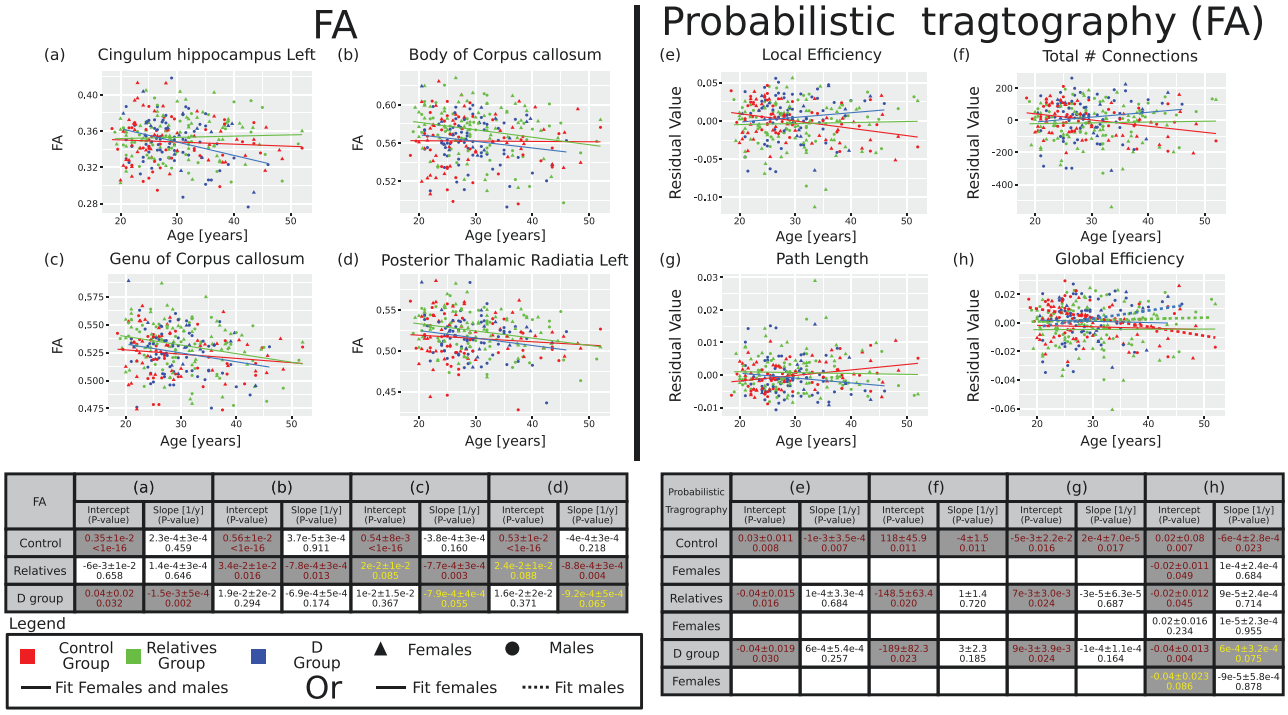

FA	(a)		(b)		(c)		(d)	
	Intercept (P-value)	Slope [1/y] (P-value)	Intercept (P-value)	Slope [1/y] (P-value)	Intercept (P-value)	Slope [1/y] (P-value)	Intercept (P-value)	Slope [1/y] (P-value)
Control	0.35±1e-2 <1e-16	2.3e-4±3e-4 0.459	0.56±1e-2 <1e-16	3.7e-5±3e-4 0.911	0.54±8e-3 <1e-16	-3.8e-4±3e-4 0.160	0.53±1e-2 <1e-16	-4e-4±3e-4 0.218
Relatives	-6e-3±1e-2 0.658	1.4e-4±3e-4 0.646	3.4e-2±1e-2 0.016	-7.8e-4±3e-4 0.013	2e-2±1e-2 0.085	-7.7e-4±3e-4 0.003	2.4e-2±1e-2 0.088	-8.8e-4±3e-4 0.004
D group	0.04±0.02 0.032	-1.5e-3±5e-4 0.002	1.9e-2±2e-2 0.294	-6.9e-4±5e-4 0.174	1e-2±1.5e-2 0.367	-7.9e-4±4e-4 0.055	1.6e-2±2e-2 0.371	-9.2e-4±5e-4 0.065

Probabilistic Tragrography	(e)		(f)		(g)		(h)	
	Intercept (P-value)	Slope [1/y] (P-value)	Intercept (P-value)	Slope [1/y] (P-value)	Intercept (P-value)	Slope [1/y] (P-value)	Intercept (P-value)	Slope [1/y] (P-value)
Control	0.03±0.011 0.008	-1e-3±3.5e-4 0.007	118±45.9 0.011	-4±1.5 0.011	-5e-3±2.2e-2 0.016	2e-4±7.0e-5 0.017	0.02±0.08 0.007	-6e-4±2.8e-4 0.023
Females							-0.02±0.011 0.049	1e-4±2.4e-4 0.684
Relatives	-0.04±0.015 0.016	1e-4±3.3e-4 0.684	-148.5±63.4 0.020	1±1.4 0.720	7e-3±3.0e-3 0.024	-3e-5±6.3e-5 0.687	-0.02±0.012 0.045	9e-5±2.4e-4 0.714
Females							0.02±0.016 0.234	1e-5±2.3e-4 0.955
D group	-0.04±0.019 0.030	6e-4±5.4e-4 0.257	-189±82.3 0.023	3±2.3 0.185	9e-3±3.9e-3 0.024	-1e-4±1.1e-4 0.164	-0.04±0.013 0.004	4e-4±2.2e-4 0.075
Females							-0.04±0.023 0.086	-9e-5±5.8e-4 0.878

Fig. 3. Slope analysis—largest scores. Four FA tracts as a function of age (a–d) and four graph matrix values from the FA along the tracts of the probabilistic tractography as a function of age (e–h) that obtained the highest epoch-averaged slope score according to the ordered from (a) to (d) for FA and (e) to (h) for the connectivity. All four connectivity measures were corrected for density and the values represent the residuals after corrections. The tables below the graphs provide fitting parameters with their *P*-values. Values in the table are for the male and females groups together (a–g) or separately when it is relevant (h). Note that for the relatives and diagnosed groups, the intercept is a relative value to the control group and not an independent number. Similarly, for females, the intercept values are relatives to the males. Slope values represent absolute values. Hence, only values for the slopes were included in the score calculations. In cases where females and males values were fitted separately, solid lines are for the females and dashed lines for the males. In brown—*P*-values below 0.05. In yellow, *P*-values between 0.05 and 0.1.

diameter and the residuals of the global efficiency, local efficiency, modularity, path length, and the number of connections after density correction showed a structural epoch-averaged age-dependency. For the diagnosed group, such functional-dependency was observed only for the diameter and the residuals of the modularity. For the relatives group, an epoch-averaged age-dependency was detected only for the diameter. The control group showed the widest level of epoch-averaged age-dependent behavior. For this group, all relevant measures besides the diameter showed epoch-averaged age-dependency.

Probabilistic Tracts Construction. The epoch-averaged slope analysis results are shown in figure S13 and Table S12 of the SI. We identified only three measures as having an epoch-averaged age-dependency and only for the females. These measures are the residuals of the assortativity, mean betweenness, and the total number of connections after density correction. For the diagnosed group, an epoch-averaged functional-dependency was detected for the residuals of the assortativity. For the control group, such functional-dependency was detected for the residuals of the mean betweenness and the total number of connections. For the relatives group, no age-dependent functional-behavior was detected.

FA Values Along Tracts Constructed by a Probabilistic Algorithm. The epoch-averaged slope analysis results are shown in figures 3e-h and Table S13 of the SI. Three measures, the residuals of the local efficiency, path length, and the total number of connections after density correction showed an epoch-averaged age-dependency. In all this cases, only the control group showed such pattern. In addition, for males, also the residuals of the global efficiency after density correction showed an epoch-averaged age-dependency for the control group (and marginally for the diagnosed group). For the relatives group no epoch-averaged age-dependency was detected.

Scoring Results. We developed a scoring system to summarize our results concisely (see "Methods" section). Scoring results are summarized in table 2. As can be seen, for Tukey's test comparison analysis, FA stood as an almost unique characteristic showing FDR corrected *q*-value below 0.05 between the relatives and some other group (mainly with the control group). An expansion of the analysis to include also tracts with

Table 1. Slope analysis of FA values

Tract	Control group		Relatives group		Diagnosed group	
FA	Slope ± SD [1/year]	*P*-value	Slope ± SD [1/year]	*P*-value	Slope ± SD [1/year]	*P*-value
Anterior corona radiata L	-8.45E-04 ± 3.41E-04	**0.0137**	-9.83E-04 ± 3.19E-04	**0.0022**	-1.00E-035.18E-04	0.0537
Anterior corona radiata R	-8.23E-04 ± 3.30E-04	**0.0132**	-6.68E-04 ± 3.08E-04	**0.0312**	-8.28E-045.01E-04	0.0998
Body of corpus callosum	-3.73E-05 ± 3.33E-04	0.9110	-7.81E-04 ± 3.11E-04	**0.0126**	-6.90E-045.06E-04	0.1737
Cingulum hippocampus L	-2.34E-04 ± 3.15E-04	0.4590	1.36E-04 ± 2.95E-04	0.6458	-1.48E-034.79E-04	**0.0022**
External capsule L	-2.43E-04 ± 2.17E-04	0.2627	-1.43E-04 ± 2.03E-04	0.4815	-6.41E-043.29E-04	0.0527
Fornix	-2.24E-03 ± 6.30E-04	**0.0004**	-1.95E-03 ± 5.89E-04	**0.0010**	-2.15E-039.57E-04	**0.0257**
Genu of corpus callosum	-3.81E-04 ± 2.70E-04	0.1600	-7.69E-04 ± 2.53E-04	**0.0026**	-7.92E-044.11E-04	0.0548
Medial lemniscus R	1.16E-03 ± 4.74E-04	**0.0150**	4.96E-04 ± 4.52E-04	0.2737	2.04E-031.11E-03	0.0688
Posterior corona radiata L	-3.44E-04 ± 2.90E-04	0.2358	-6.25E-04 ± 2.71E-04	**0.0217**	-7.47E-044.40E-04	0.0904
Posterior limb of internal capsule L	-6.94E-04 ± 3.84E-04	0.0716	-1.01E-033.52E-04	**0.0044**	-7.00E-044.48E-04	0.1192
Posterior limb of internal capsule R	-7.79E-04 ± 3.72E-04	**0.0370**	-1.00E-033.41E-04	**0.0036**	-4.93E-044.34E-04	0.2565
Posterior thalamic radiation L	-4.03E-04 ± 3.26E-04	0.2182	-8.82E-043.05E-04	**0.0041**	-9.18E-044.95E-04	**0.0650**
Posterior thalamic radiation R	-9.27E-04 ± 5.17E-04	0.0741	-8.88E-044.75E-04	0.0625	-8.77E-046.04E-04	0.1472
Posterior thalamic radiation R	-4.86E-04 ± 4.59E-04	0.2901	-1.01E-034.38E-04	**0.0218**	-5.05E-041.08E-03	0.6400
Retrolenticular part of internal capsule L	-1.47E-04 ± 3.98E-04	0.7115	-4.29E-053.80E-04	0.9101	-1.65E-039.37E-04	0.0797
Retrolenticular part of internal capsule R	-7.55E-04 ± 4.51E-04	0.0951	-1.15E-034.14E-04	**0.0057**	-6.67E-045.26E-04	0.2061
Sagittal stratum L	-2.28E-04 ± 3.94E-04	0.5633	-4.72E-043.61E-04	0.1929	-8.26E-044.59E-04	0.0732
Sagittal stratum L	-6.15E-04 ± 3.49E-04	0.0789	-3.21E-043.33E-04	0.3353	-1.47E-038.21E-04	0.0743
Sagittal stratum R	-4.63E-04 ± 4.19E-04	0.2702	-8.71E-043.85E-04	**0.0243**	-9.92E-044.89E-04	**0.0435**
Superior longitudinal fasciculus R	-5.26E-04 ± 2.78E-04	0.0595	8.25E-052.60E-04	0.7507	-1.93E-044.22E-04	0.6486

Note: Values represent the fitting slope parameters obtained from fitting the FA value as a function of age for the whole group (black), males (red), or females (blue). Bold—slope fitting *P*-value below 0.05. Underline—slope fitting *P*-value between 0.05 and 0.1.
L, left hemisphere, R, right hemisphere.

FDR corrected value below 0.1 showed similar pattern (see table 2). Similarly, for the epoch-averaged slope analysis, only for AD and RD, the scoring system supports a naive 'Familial Risk' model where the value of the relatives group is intermediate between that of the control and that of the diagnosed groups. By contrast, the relatives' group showed either the most or the least epoch-averaged age-dependent behavior relative to the two other groups for FA, MD, and three of the four connectivity modalities.

Longitudinal Data Analysis. For the diffusivity measures, the longitudinal analysis did not provide a substantial indication for an Age*Group dependency. See figures S14, S15, and the Supporting Text in the SI.

No indication of longitudinal Age*Group was detected for the deterministic and probabilistic connectivity.

For the connectivity of the FA along the tracts calculated using the deterministic algorithm, several measures had a *q*-value below 0.05 when comparing a linear mixed model with an Age*Group fixed-effect relative to a model without this factor. These measures are the local efficiency, path length, and the number of connections. In addition, the global efficiency and the modularity had a *q*-value between 0.05 and 0.1. For the connectivity of the FA along the tracts calculated using the probabilistic algorithm, the results were similar, but the mean participation coefficients also showed a *q*-value between 0.05 and 0.1. However, for all these measures besides the local efficiency, we noticed lower values of the measures for the first epoch of the study relative to the other two epochs. Hence, the hetero-skedasticity of the linear mixed model was not maintained, and the results cannot be trusted.

Results of the longitudinal local efficiency for the FA along the tracts are shown in figure 4 for the probabilistic algorithm and figure S16 of the SI for the deterministic algorithm. As can be seen, incorporating the Age*Group fixed effect improved the model predictions mainly for the control and diagnosed group but not for the relative group. Interestingly, in this case, as can be seen from the tables below the figures, the longitudinal age-dependency was most pronounced for the difference between the control and diagnosed groups. In contrast, the relatives group showed a longitudinal age-dependency intermediate between the other two groups. However, this effect was minimal, less than one percent of the local efficiency absolute value. It was also not detected when comparing the Δ values between the different epochs using a Tukey's test for the probabilistic analysis and only rarely for the deterministic analysis (results not shown, see "Method"

Table 2. Scores of the three groups comparison

	Tukey's test comparisons			Slope analysis		
	C-D	R-D	C-R	C	R	D
FA	0	0.050 ± 0.013 (0.075 ± 0.012)	**0.057 ± 0.007 (0.623 ± 0.018)**	0.188 ± 0.013	**0.451 ± 0.023**	0.282 ± 0.023
MD	0	0	0	0048 ± 0.016	0.033 ± 0.016	**0.092 ± 0.021**
AD	0	0	0	**0.261 ± 0.015**	0.128 ± 0.014	0.052 ± 0.008
RD	0	0	0	0.057 ± 0.016	0.131 ± 0.036	**0.156 ± 0.035**
Deterministic connectivity	**0.155 ± 0.026**	0	0	**0.100****	0*	0*
Deterministic connectivity—FA along tracts probabilistic	0	0	0	**0.332 ± 0.043**	0.039 ± 0.016	0.094 ± 0.024
Probabilistic connectivity	0	0	0	**0.066 ± 0.026**	0*	0.004 ± 0.002
Probabilistic connectivity—FA along tracts	0	0	0	**0.285 ± 0.035**	0*	0.006 ± 0.003

Note: Scores were calculated as is described in the "Methods" section. C-D—aggregate comparison between the control and the diagnosed groups. R-D—aggregate comparison between the relatives and diagnosed groups. C-R—aggregate comparison between the control and relatives groups. C—control group. R - Relatives group. D—diagnosed group. For Tukey's test comparisons analysis, bold represents the largest value. For FA the value in the parenthesis represent similar analysis to the score analysis but including all tracts with FDR corrected q-value below 0.1 instead of 0.05. In this case, the formula for calculating the score was adjusted accordingly, replacing the value 0.05 by 0.1 (see "Methods" section). For the epoch-averaged slope analysis, bold represents the largest value, and an underline the smallest. *Standard deviation (SD) could not be calculated since all values are 0. **SD could not be calculated since there is only one value.

section). Hence, these results should be taken with caution.

Discussion

In this study, we showed a putative WM-based structural compensation mechanism in the brain of relatives. Such a mechanism might protect the relatives group against the deleterious load associated with their genetic background. We inferred such a putative compensation mechanism based on the scoring results of Tukey's test analysis for FA and the epoch-averaged scoring results for the age-dependent slope for diffusivity and connectivity. In the last case, the relatives' group often showed the most or the least epoch-averaged age-dependent change.

In particular, in Tukey's test epoch-averaged analysis, six tracts showed such unique behavior for the relatives group (see "Results" section). Previously, some of these tracts were implicated in the pathophysiology of psychosis or as a risk factor for psychosis.[40] From the FA epoch-averaged age-dependent slope, tracts that show unique behavior for the relatives group (for females, males, or females and males together) were the left posterior corona radiata, left posterior thalamic radiation, right posterior thalamic radiation, right retrolenticular part of the internal capsule, and left sagittal stratum. For the AD, these tracts were the right cerebral peduncle, left medial lemniscus, and left superior fronto occipital fasciculus. For the RD, it was the Genu of corpus callosum.

Concerning connectivity, the control group showed an epoch-average slope dependency for some measures, especially for the local efficiency, path length, and the number of connections. The relatives and diagnosed groups did not show such a pattern. By contrast, there were measures where the diagnosed group also showed epoch-average slope dependency, while the relatives did not. These measures were, for example, modularity (deterministic FA along tracts), assortativity (probabilistic tractography for females), or global efficiency (probabilistic FA along tracts for males). Hence, overall, the relatives group showed the least epoch-averaged age-dependency over three of the four modes of analysis.

Years of studies suggested group-level gray matter abnormalities in the brain of people diagnosed with psychosis.[41,42] Accumulated evidence from DTI studies also shows group-level white matter (WM) abnormalities for the same group, mainly concerning the FA.[43–46] Structural connectivity studies suggested a similar pattern concerning measures of brain segregation and integration.[47] These structural abnormalities are suspected to be related to the negative, positive and cognitive symptoms associated with psychosis.[48]

The previously published results in the scientific literature are a bit more complex for relatives of people diagnosed with psychosis. On the one hand, there is widespread evidence for gray matter,[49] WM,[1,40] functional connectivity,[50–52] and task-based functional analysis[53,54] abnormalities that support the "Familial Risk" model.

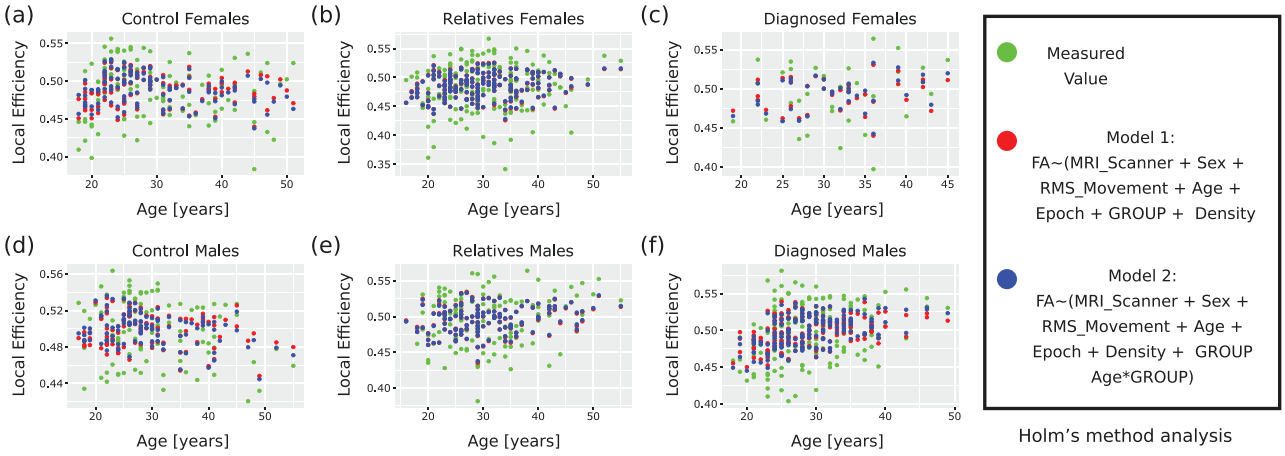

Model	# of parameters	AIC	BIC	Log Likelihood	deviance	χ2	Probavility (>χ2)
●	13	-2860.2	-2800.7	1443.1	-2886.2		
●	15	-2866.9	-2798.3	1448.5	-2896.9	10.747	0.005

Holm's method analysis

Age* GROUP	Value	χ2	Probavility (>χ2)
C-D	-1.7e-3	10.404	0.038
C-R	-8.5e-4	4.149	0.083
D-R	8.9e-4	2.887	0.089

Fig. 4. Longitudinal analysis of local efficiency obtained from sampling the FA values along the probabilistic connectivity tracts. Longitudinal analysis of the local efficiency, the only reliable measure that showed an FDR corrected ANOVA *q*-value below 0.05 when comparing two linear mixed models. Model (a) in R notation—Local_Efficiency ~ (MRI_Scanner + Sex + RMS_Movement + Age + Epoch + Density + GROUP) + (1 | Family:Subject). Model (b) in R notation—Local_Efficiency ~ (MRI_Scanner + Sex + RMS_Movement + Age + Epoch + Density + GROUP + Age*GROUP) + (1|Family:Subject). (a–c) graphs for females. (d–f) graphs for males. (a, d)—Control group. (b, e)—Relatives group. (c, f)—Diagnosed group. Green dots are the actual values measured (along all three epochs of the study). Red dots are the predictions of model (a). Blue dots are the predictions of model (b). When no red dot is seen, it means that the prediction of model (a) and model (b) were indistinguishable. The tables below the graphs show the ANOVA results between the two models, the Age*GROUP χ^2, and the Holm's method analysis of the Age*GROUP factor. AIC, akaike information criterion; BIC, Bayesian Information Criterion; C-D, difference between the control and D groups; C-R, difference between the control and relatives groups; D-R, difference between the D and relatives groups (note that in this case, C-D and similar notations represent a minus sign, unlike Tukey's test case).

On the other hand, some evidence also suggests unique features of the relatives compared to both the control and the probands groups concerning the gray matter development during adolescence,[55,56] gray matter level during adulthood,[57,58] and functional brain activity.[59] When such unique features are found, it is interesting to interpret these features as representing compensation or resilience mechanism as was done in the context of some psychiatric conditions.[60] Following this logic, we interpret our finding in that direction.

It is well-known that in findings concerning brain features in psychosis among probands, the effect sizes are usually small to medium. Similar, or smaller, effect sizes are also found among relatives. Consequently, it is relatively hard to identify unique or psychopathological features of these groups in neuroimaging studies. To tackle this obstacle, we have used two strategies. First, to reduce the possibility of a regression to the mean, we studied epoch-averaged values of three separate measurements. Second, we aggregated our results using a single score analysis to obtain an overall picture of the group comparison. Hence, instead of pointing at specific tracts or connectivity features unique to the relatives' group, we would like to point to the aggregated unique epoch-averaged findings among the relatives group and the general idea of a compensation mechanism. Further research in that direction is essential since some WM abnormalities among the diagnosed group might represent pathophysiological processes rather than a pre-condition.[61]

Note that the previous GROUP cohort work suggested a WM "Familial Risk" model concerning some brain features.[62–64] However, in other studies from the same cohort, when assessing other brain features, the relatives did not show statistically significant differences compared to the control group.[30,65,66] A similar conclusion concerning structural connectivity was also obtained in another site of the GROUP cohort.[64] Yet, in other cases from the GROUP cohort, a unique behavior of some relatives' brain features was observed.[31,67] Finally, several psychological resilience factors among patients or relatives were identified through research in the GROUP cohort.[68,69] Hence, it is also consistent to say that the GROUP cohort does not fully support the "Familial Risk" model.

When assessing the current study, it is important to recall that it has several limitations. First, it is based on scanners with relatively low field strength, which makes it hard to track crossing fibers. Second, overall the size of the analyzed cohort is only of a medium to small size. Third, the current cohort includes mainly young-adulthood individuals and does not assess

developmental or aging processes. Fourth, it is known that psychosis is a diverse condition with many different sub-types.[70] Hence, it is hard to infer from this cohort for other populations. Fifth, it is known that different choices of the parcellations atlas can influence MRI analysis results.[71] Sixth and importantly, the percentage of males and females is not equal between the three groups. In particular, there are many more males than females among the people diagnosed with psychosis compared to the other two groups. We have tried to control for this factor at various analysis steps (see "Methods" section). Nevertheless, a better study design would have been achieved if the number of females and males in the three groups had been balanced and equal already during the data acquisition stage.

In light of these limitations, it is clear that our study will need further replication and might represent a unique feature of the GROUP cohort. We also suggest taking our results with a cautionary note, especially when it comes to the idea of an inverse U-shape relationship between genetic liability to psychosis and brain functioning.[72] Nevertheless, this study can contribute to the developing idea of compensation (or protective) mechanisms in the brain of the relatives group.

Supplementary Material

Supplementary data are available at *Schizophrenia Bulletin Open* online.

Acknowledgments

This work was supported by the Netherlands Organization for Scientific Research (NWO 184.033.111), Biobanking and BioMolecular resources Research Infrastructure The Netherlands (BBMRI-NL2.0), and by the ENIGMA World Aging Center grant (NIH 1R56AG058854-01, subaward 112068003). The GROUP study is funded through the Geestkracht programme of the Dutch Health Research Council (Zon-Mw, grant number 10-000- 1001).

Conflict of interest statement

All authors declare no conflict of interests.

Author contributions

YC conceived the study, developed the pipleline, preformed the experiment, analyzed the data, inferred conclusions, and wrote the article.

References

1. Skudlarski P, Schretlen DJ, Thaker GK, *et al.* Diffusion tensor imaging white matter endophenotypes in patients with schizophrenia or psychotic bipolar disorder and their relatives. *Am J Psychiatry.* 2013;170(8):886–898.
2. de Zwarte SMC, Brouwer RM, Tsouli A, *et al.* Running in the family? Structural brain abnormalities and IQ in offspring, siblings, parents, and co-twins of patients with schizophrenia. *Schizophr Bull.* 2018;45(6):1209–1217.
3. Lichtenstein P, Yip BH, Björk C, *et al.* Common genetic determinants of schizophrenia and bipolar disorder in Swedish families: a population-based study. *Lancet* 2009;373(9659):234–239.
4. Hilker R, Helenius D, Fagerlund B, *et al.* Heritability of schizophrenia and schizophrenia spectrum based on the Nationwide Danish Twin Register. *Biol Psychiatry.* 2018;83(6):492–498.
5. Kyaga S, Lichtenstein P, Boman M, Hultman C, Långström N, Landén M. Creativity and mental disorder: family study of 300 000 people with severe mental disorder. *Br J Psychiatry.* 2011;199(5):373–379.
6. Power RA, Steinberg S, Bjornsdottir G, *et al.* Polygenic risk scores for schizophrenia and bipolar disorder predict creativity. *Nat Neurosci.* 2015;18(7):953–955.
7. Muñoz Maniega S, Lymer G, Bastin M, *et al.* A diffusion tensor MRI study of white matter integrity in subjects at high genetic risk of schizophrenia. *Schizophr Res.* 2008;106(2–3):132–139.
8. Hao Y, Yan Q, Liu H, *et al.* Schizophrenia patients and their healthy siblings share disruption of white matter integrity in the left prefrontal cortex and the hippocampus but not the anterior cingulate cortex. *Schizophr Res.* 2009;114(1–3):128–135.
9. Collin G, Hulshoff Pol HE, Haijma SV, Cahn W, Kahn RS, van den Heuvel MP. Impaired cerebellar functional connectivity in schizophrenia patients and their healthy siblings. *Front Psychiatry.* 2011;2:73. doi:10.3389/fpsyt.2011.00073.
10. Bohlken MM, Brouwer RM, Mandl RCW, *et al.* Structural brain connectivity as a genetic marker for schizophrenia. *JAMA Psychiatry.* 2016;73(1):11–19. doi:10.1001/jamapsychiatry.2015.1925.
11. de Zwarte SMC, Brouwer RM, Agartz I, *et al.* The association between familial risk and brain abnormalities is disease specific: an ENIGMA-relatives study of schizophrenia and bipolar disorder. *Biol Psychiatry.* 2019;86(7):545–556.
12. Knöchel C, Oertel-Knööchel V, Schönmeyer R, *et al.* Interhemispheric hypoconnectivity in schizophrenia: fiber integrity and volume differences of the corpus callosum in patients and unaffected relatives. *Neuroimage.* 2012;59(2):926–934.
13. Cho KIK, Kim M, Yoon YB, Lee J, Lee TY, Kwon JS. Disturbed thalamocortical connectivity in unaffected relatives of schizophrenia patients with a high genetic loading. *Aust N Z J Psychiatry.* 2019;53(9):889–895.
14. O'Hanlon E, Leemans A, Kelleher I, *et al.* White matter differences among adolescents reporting psychotic experiences. *JAMA Psychiatry.* 2015;72(7):668–677. doi:10.1001/jamapsychiatry.2015.0137.
15. Saito J, Hori M, Nemoto T, *et al.* Longitudinal study examining abnormal white matter integrity using a tract-specific analysis in individuals with a high risk for psychosis. *Psychiatry Clin Neurosci.* 2017;71(8):530–541.
16. Oestreich LKL, Randeniya R, Garrido MI. White matter connectivity reductions in the pre-clinical continuum of psychosis: a connectome study. *Hum Brain Mapp.* 2018;40(2):529–537.
17. Mizuno Y, Wartelsteiner F, Frajo-Apor B. Resilience research in schizophrenia. *Curr Opin Psychiatry.* 2016;29(3):218–223.

18. Kalisch R, Baker DG, Basten U, *et al.* The resilience framework as a strategy to combat stress-related disorders. *Nat Hum Behav.* 2017;1(11):784–790.
19. Dazzan P. Not just risk: there is also resilience and we should understand its neurobiological basis. *Schizophr Res.* 2018;193:293–294. doi:10.1016/j.schres.2017.08.021.
20. Hess JL, Tylee DS, Mattheisen M, *et al.* A polygenic resilience score moderates the genetic risk for schizophrenia. *Mol Psychiatr.* 2021;26(3):800–815.
21. Van der Auwera S, Wittfeld K, Shumskaya E, *et al.* Predicting brain structure in population-based samples with biologically informed genetic scores for schizophrenia. *Am J Med Genet B Neuropsychiatr Genet.* 2017;174(3):324–332.
22. Reus LM, Shen X, Gibson J, *et al.* Association of polygenic risk for major psychiatric illness with subcortical volumes and white matter integrity in UK Biobank. *Sci Rep.* 2017;7(1):42140. doi:10.1038/srep42140.
23. Simões B, Vassos E, Shergill S, *et al.* Schizophrenia polygenic risk score influence on white matter microstructure. *J Psychiatr Res.* 2020;121:62–67. doi:10.1016/j.jpsychires.2019.11.011.
24. Alloza C, Cox SR, Blesa Cábez M, *et al.* Polygenic risk score for schizophrenia and structural brain connectivity in older age: a longitudinal connectome and tractography study. *Neuroimage.* 2018;183:884–896. doi:10.1016/j.neuroimage.2018.08.075.
25. Hpptman M, Nierenberg J, Bertisch H, *et al.* A DTI study of white matter microstructure in individuals at high genetic risk for schizophrenia. *Schizophr Res.* 2008;106(2–3):115–124.
26. Ganella EP, Seguin C, Bartholomeusz CF, *et al.* Risk and resilience brain networks in treatment-resistant schizophrenia. *Schizophr Res.* 2018;193:284–292. doi:10.1016/j.schres.2017.07.014.
27. Wei Q, Zhao L, Zou Y, *et al.* The role of altered brain structural connectivity in resilience, vulnerability, and disease expression to schizophrenia. *Prog Neuropsychopharmacol Biol Psychiatry.* 2020;101:109917. doi:10.1016/j.pnpbp.2020.109917.
28. de Leeuw M, Bohlken MM, Mandl RCW, Hillegers MHJ, Kahn RS, Vink M. Changes in white matter organization in adolescent offspring of schizophrenia patients. *Neuropsychopharmacology.* 2017;42:495–501. doi:10.1038/npp.2016.130.
29. Bolhuis K, Tiemeier H, Jansen PR, *et al.* Interaction of schizophrenia polygenic risk and cortisol level on pre-adolescent brain structure. *Psychoneuroendocrinology.* 2019;101:295–303. doi:10.1016/j.psyneuen.2018.12.231.
30. Boos HBM, Mandl RCW, van Haren NEM, *et al.* Tract-based diffusion tensor imaging in patients with schizophrenia and their non-psychotic siblings. *Eur Neuropsychopharm.* 2013;23(4):295–304.
31. Chang X, Mandl RCW, Pasternak O, Brouwer RM, Cahn W, Collin G. Diffusion MRI derived free-water imaging measures in patients with schizophrenia and their non-psychotic siblings. *Prog Neuropsychopharmacol Biol Psychiatry.* 2021;109:110238. doi:10.1016/j.pnpbp.2020.110238.
32. Vettel JM, Cooper N, Garcia JO, Yeh FC, Verstynen TD. White matter tractography and diffusion-weighted imaging. In: *ELS*. Hoboken, NJ: John Wiley & Sons, Ltd; 2017:1–9. doi:10.1002/9780470015902.a0027162
33. Korver N, Quee PJ, Boos HBM, Simons CJP, de Haan L. Genetic Risk and Outcome of Psychosis (GROUP), a multi site longitudinal cohort study focused on gene-environment interaction: objectives, sample characteristics, recruitment and assessment methods. *Int J Methods Psychiatr Res.* 2012;21(3):205–221.
34. Rubinov M, Sporns O. Complex network measures of brain connectivity: uses and interpretations. *Neuroimage.* 2010;52(3):1059–1069.
35. van den Heuvel MP, Mandl RCW, Stam CJ, Kahn RS, Hulshoff Pol HE. Aberrant frontal and temporal complex network structure in schizophrenia: a graph theoretical analysis. *J Neurosci.* 2010;30(47):15915–15926.
36. Drakesmith M, Caeyenberghs K, Dutt A, *et al.* Schizophrenia-like topological changes in the structural connectome of individuals with subclinical psychotic experiences. *Hum Brain Mapp.* 2015;36(7):2629–2643.
37. Team RC. *R: A Language and Environment for Statistical Computing*. Vienna, Austria: R Foundation for Statistical Computing; 2020. https://www.R-project.org/. Accessed October 6, 2022.
38. Krishnan A, Williams LJ, McIntosh AR, Abdi H. Partial Least Squares (PLS) methods for neuroimaging: a tutorial and review. *Neuroimage.* 2011;56(2):455–475.
39. van Dellen E, Bohlken MM, Draaisma L, *et al.* Structural brain network disturbances in the psychosis spectrum. *Schizophr Bull.* 2015;42(3):782–789.
40. Merritt K, Luque Laguna P, Irfan A, David AS. Longitudinal structural MRI findings in individuals at genetic and clinical high risk for psychosis: a systematic review. *Front Psychiatry.* 2021;12:620401. doi:10.3389/fpsyt.2021.620401.
41. Thermenos HW, Keshavan MS, Juelich RJ, *et al.* A review of neuroimaging studies of young relatives of individuals with schizophrenia: a developmental perspective from schizotaxia to schizophrenia. *Am J Med Genet B Neuropsychiatr Genet.* 2013;162(7):604–635.
42. van Erp TGM, Hibar DP, Rasmussen JM, *et al.* Subcortical brain volume abnormalities in 2028 individuals with schizophrenia and 2540 healthy controls via the ENIGMA consortium. *Mol Psychiatry.* 2015;21(4):547–553.
43. Kelly S, Jahanshad N, Zalesky A, *et al.* Widespread white matter microstructural differences in schizophrenia across 4322 individuals: results from the ENIGMA Schizophrenia DTI Working Group. *Mol Psychiatry.* 2017;23(5):1261–1269.
44. Yang X, Cao D, Liang X, Zhao J. Schizophrenia symptomatic associations with diffusion tensor imaging measured fractional anisotropy of brain: a meta-analysis. *Neuroradiology.* 2017;59(7):699–708.
45. Cetin-Karayumak S, Di Biase MA, Chunga N, *et al.* White matter abnormalities across the lifespan of schizophrenia: a harmonized multi-site diffusion MRI study. *Mol Psychiatry.* 2019;25(12):3208–3219.
46. Karlsgodt KH. White matter microstructure across the psychosis spectrum. *Trends Neurosci.* 2020;43(6):406–416.
47. Collin G, van den Heuvel MP. Anatomical and functional brain network architecture in schizophrenia. In: Abel T, Nickl-Jockschat T, eds. *The Neurobiology of Schizophrenia*. Amsterdam, Netherlands: Elsevier; 2016:313–336. doi:10.1016/b978-0-12-801829-3.00026-4.
48. Sheffield JM, Barch DM. Cognition and resting-state functional connectivity in schizophrenia. *Neurosci Biobehav Rev.* 2016;61:108–120. doi:10.1016/j.neubiorev.2015.12.007.
49. Boos HBM, Aleman A, Cahn W, Pol HH, Kahn RS. Brain volumes in relatives of patients with schizophrenia. *Arch Gen Psychiatry.* 2007;64(3):297–304. doi:10.1001/archpsyc.64.3.297.

50. Lo CYZ, Su TW, Huang CC, *et al.* Randomization and resilience of brain functional networks as systems-level endophenotypes of schizophrenia. *Proc Natl Acad Sci.* 2015;112(29):9123–9128.
51. Duan J, Xia M, Womer FY, *et al.* Dynamic changes of functional segregation and integration in vulnerability and resilience to schizophrenia. *Hum Brain Mapp.* 2019;40(7):2200–2211.
52. Xi C, Liu ZN, Yang J, *et al.* Schizophrenia patients and their healthy siblings share decreased prefronto-thalamic connectivity but not increased sensorimotor-thalamic connectivity. *Schizophr Res.* 2020;222:354–361. doi:10.1016/j.schres.2020.04.033.
53. Braun U, Schäfer A, Bassett DS, *et al.* Dynamic brain network reconfiguration as a potential schizophrenia genetic risk mechanism modulated by NMDA receptor function. *Proc Natl Acad Sci.* 2016;113(44):12568–12573.
54. Zhang R, Picchioni M, Allen P, Toulopoulou T. Working memory in unaffected relatives of patients with schizophrenia: a meta-analysis of functional magnetic resonance imaging studies. *Schizophr Bull.* 2016;42(4):1068–1077.
55. Moran ME, Hulshoff Pol H, Gogtay N. A family affair: brain abnormalities in siblings of patients with schizophrenia. *Brain.* 2013;136(11):3215–3226.
56. Zalesky A, Pantelis C, Cropley V, *et al.* Delayed development of brain connectivity in adolescents with schizophrenia and their unaffected siblings. *JAMA Psychiatry.* 2015;72(9):900–908. doi:10.1001/jamapsychiatry.2015.0226.
57. Zhang W, Lei D, Keedy SK, *et al.* Brain gray matter network organization in psychotic disorders. *Neuropsychopharmacology.* 2019;45(4):666–674.
58. Zhang W, Sweeney JA, Yao L, *et al.* Brain structural correlates of familial risk for mental illness: a meta-analysis of voxel-based morphometry studies in relatives of patients with psychotic or mood disorders. *Neuropsychopharmacology.* 2020;45(8):1369–1379.
59. Saarinen AIL, Huhtaniska S, Pudas J, *et al.* Structural and functional alterations in the brain gray matter among first-degree relatives of schizophrenia patients: a multimodal meta-analysis of fMRI and VBM studies. *Schizophr Res.* 2020;216:14–23. doi:10.1016/j.schres.2019.12.023.
60. Frangou S. Neuroimaging markers of risk, disease expression, and resilience to bipolar disorder. *Curr Psychiatry Rep.* 2019;21(7):52. doi:10.1007/s11920-019-1039-7.
61. Xiao Y, Sun H, Shi S, *et al.* White matter abnormalities in never-treated patients with long-term schizophrenia. *Am J Psychiatry.* 2018;175(11):1129–1136.
62. Collin G, Kahn RS, de Reus MA, Cahn W, van den Heuvel MP. Impaired rich club connectivity in unaffected siblings of schizophrenia patients. *Schizophr Bull.* 2013;40(2):438–448.
63. de Leeuw M, Bohlken MM, Mandl RCW, Kahn RS, Vink M. Reduced fronto–striatal white matter integrity in schizophrenia patients and unaffected siblings: a DTI study. *Npj Schizophr.* 2015;1(1):15001. doi:10.1038/npjschz.2015.1.
64. Michielse S, Rakijo K, Peeters S, Viechtbauer W, van Os J, Marcelis M. Microstructural white matter network-connectivity in individuals with psychotic disorder, unaffected siblings and controls. *NeuroImage Clin.* 2019;23:101931. doi:10.1016/j.nicl.2019.101931.
65. Boos HBM, Cahn W, van Haren NEM, *et al.* Focal and global brain measurements in siblings of patients with schizophrenia. *Schizophr Bull.* 2011;38(4):814–825.
66. Chang X, Collin G, Mandl RCW, Cahn W, Kahn RS. Interhemispheric connectivity and hemispheric specialization in schizophrenia patients and their unaffected siblings. *NeuroImage Clin.* 2019;21:101656. doi:10.1016/j.nicl.2019.101656.
67. Domen P, Peeters S, Michielse S, *et al.* Differential time course of microstructural white matter in patients with psychotic disorder and individuals at risk: a 3-year follow-up study. *Schizophr Bull.* 2016;43(1):160–170.
68. Schirmbeck F, Boyette LL, Valk R van der, *et al.* Relevance of five-factor model personality traits for obsessive–compulsive symptoms in patients with psychotic disorders and their un-affected siblings. *Psychiatry Res.* 2015;225(3):464–470.
69. van Zelst C, van Nierop M, van Dam DS, Bartels-Velthuis AA, Delespaul P. Associations between stereotype awareness. Childhood trauma and psychopathology: a study in people with psychosis, their siblings and controls. *Plos One.* 2015;10(2):e0117386. doi:10.1371/journal.pone.0117386.
70. Karlsgodt KH. Diffusion imaging of white matter in schizophrenia: progress and future directions. *Biol Psychiatry Cogn Neurosci Neuroimaging.* 2016;1(3):209–217.
71. de Reus MA, van den Heuvel MP. The parcellation-based connectome: limitations and extensions. *Neuroimage.* 2013;80:397–404. doi:10.1016/j.neuroimage.2013.03.053.
72. Abraham A. Editorial: madness and creativity—yes, no or maybe? *Front Psychol.* 2015;6:1055. doi:10.3389/fpsyg.2015.01055.
73. Jenkinson M, Beckmann CF, Behrens TEJ, Woolrich MW, Smith SM. FSL. *Neuroimage.* 2012;62(2):782–790.
74. Tournier JD, Smith R, Raffelt D, *et al.* MRtrix3: a fast, flexible and open software framework for medical image processing and visualisation. *Neuroimage.* 2019;202:116137. doi:10.1016/j.neuroimage.2019.116137.
75. Desikan RS, Ségonne F, Fischl B, *et al.* An automated labeling system for subdividing the human cerebral cortex on MRI scans into gyral based regions of interest. *Neuroimage.* 2006;31(3):968–980.
76. Glasser MF, Coalson TS, Robinson EC, *et al.* A multimodal parcellation of human cerebral cortex. *Nature.* 2016;536(7615):171–178.